THE JOURNAL OF NAVIGATION (2016), **69**, 1097–1113.
doi:10.1017/S0373463315001058

Development and Performance Validation of a Navigation System for an Underwater Vehicle

R. Ramesh, V. Bala Naga Jyothi, N. Vedachalam, G.A. Ramadass and M.A. Atmanand

(*National Institute of Ocean Technology, Ministry of Earth Sciences, Chennai, India*)
(E-mail: rramesh@niot.res.in)

Underwater position data is a key requirement for the navigation and control of unmanned underwater vehicles. The proposed navigation scheme can be used in any vessel or boat for any shallow water vehicle. This paper presents the position estimation algorithm developed for shallow water Remotely Operated Vehicles (ROVs) using attitude data and Doppler Velocity Log data with the initial position from the Global Positioning System (GPS). The navigational sensors are identified using the in-house developed simulation tool in MATLAB, based on the requirement of a position accuracy of less than 5%. The navigation system is built using the identified sensors, Kalman filter and navigation algorithm, developed in LabVIEW software. The developed system is tested and validated for position estimation, with an emulator consisting of a GPS-aided fibre optic gyro-based inertial navigation system as a reference, and it is found that the developed navigation system has a position error of less than 5%.

KEYWORDS

1. Emulator. 2. Doppler Velocity Log. 3. Position estimation. 4. Remotely Operated Vehicle.

Submitted: 21 February 2015. Accepted: 11 December 2015. First published online: 26 January 2016.

1. INTRODUCTION. Underwater vehicles require precision navigational sensors for the purpose of effective navigation and to determine the position of the vehicle in real time. The precision requirement depends on the mission objectives, sensor accuracies and duration (Ramadass et al., 2013; Geng et al., 2010; Li and Wang, 2013). Manned and unmanned underwater vehicles designed for complex subsea operations and long mission durations are often equipped with very high precision Fibre Optic Gyro (FOG)-based Inertial Navigation Systems (INS), aided by a Doppler Velocity Log (DVL) and acoustic base line positioning systems (Vedachalam et al., 2014a; Narayanaswamy et al., 2013; Vedachalam et al., 2014b). Shallow water vehicles, which are designed for shorter mission periods, are often fitted with a navigational system comprising MEMS (Micro-Electro-Mechanical Systems)/magnetic sensor technology-based attitude sensors (Fossen, 2012), DVL and a processor for real time

computation of the position. The navigation system is initialised with a position input from an external terrestrial Global Positioning System (GPS) and works in a dead reckoning mode (Marco and Healey, 2001) during the underwater mission. In the dead reckoning mode, based on the last known or computed position, the navigational algorithm estimates the current position based on the inputs from the sensor suite. The sensor suite comprises attitude sensors measuring the vehicle's orientation in three Degrees Of Freedom (DOF) and the acoustic-based DVL measures the vehicle's body frame linear velocities in all three axes.

The precision of the sensor hardware suite and the effectiveness of the position estimation algorithm are vital in effective position determination. The selection of the sensor suite is a trade-off between the position estimation needs of the mission, sensor footprint and costs (Grewal et al., 2001; Ellingsen, 2008). The National Institute of Ocean Technology (NIOT) designed and developed a Remotely Operated Vehicle (ROV) with a depth rating of 500 m for shallow water and polar exploration. This paper presents the development of an INS for the shallow water ROV which can be deployed from any ship. The selection of the navigation sensor suite is done with the aid of the in-house developed simulator tool, which is a MATLAB mathematical model that takes the sensor error model parameters and user-defined mission profile as inputs, and simulates the vehicle trajectory in geo-coordinates. The tool also displays the vehicle trajectory under ideal sensor conditions for the same mission profile. Based on the simulation results obtained for various combinations of sensors and the mission target position accuracy requirement of less than 5%, the attitude sensor and DVL hardware are realised. A real time controller and LabVIEW software are used for data acquisition and algorithm development for computing the position with the Kalman filter. Prior to installing the systems on board the ROV, the calibration of the inertial and attitude sensor has been carried out as per the recommended calibration procedures given by the manufacturer. Calibration of the Photonic Inertial Navigation System (PHINS) was performed with the aid of GPS, as per the instruction given in the user manual (PHINS, 2013). A staircase shaped trajectory was performed during the fine alignment mode until the heading covariance was less than 0·1°. With this, the developed navigational system is validated for the desired performance, using an in-house developed emulator (which is based on the GPS-aided high precision FOG-based INS and error models of the sensors), which provides the attitude and velocity sensor inputs, with accuracies resembling the selected sensor suite and validated on board a terrestrial vehicle, with a mission profile closely resembling the actual underwater vehicle. The developed system is installed and qualified for the desired performance on board the NIOT developed 500 m depth rated ROV.

2. POSITION ESTIMATION METHODOLOGY IN UNDERWATER VEHICLES.

Land-based and ocean surface vessel navigational systems utilise GPS signals for computing their position (Hegrenaes et al., 2008). GPS signals cannot be used by underwater vehicles as electromagnetic waves suffer significant attenuation in water (Fallon et al., 2010). Prior to deployment, the underwater vehicle navigational system is initialised with the position input from the external GPS. It then works in the dead reckoning mode during the underwater mission. In the dead reckoning mode, based on the last known or computed position, the navigational

https://doi.org/10.1017/S0373463315001058 Published online by Cambridge University Press

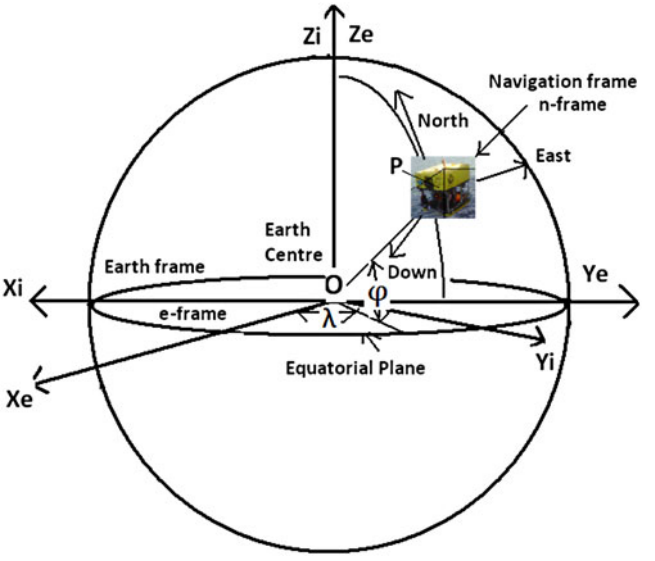

Figure 1. Vehicle orientation in the Earth frame.

algorithm, with inputs from the vehicle on board attitude sensors and DVL, estimates the current position. The DVL, which is mounted on the body frame of the vehicle, measures the vehicle velocity in body frame coordinates (Jalving et al., 2003). In order to compute the change in position of the navigating vehicle with respect to the Earth frame, the measured body frame velocity needs to be converted into an Earth frame. Figure 1 represents the vehicle with reference to the Earth frame, where the velocities are to be resolved in the North and East directions and Figure 2 represents the six DOF parameters for a typical ROV in the body frame.

The conversion of the DVL measured body frame velocity to an Earth frame velocity is achieved using the Direct Cosine Matrix (DCM) transformation with the vehicle attitude parameters (Fossen, 1994; Hofmann-Wellenhof et al., 2011; Hegrenaes et al., 2008) represented in Equation (1).

$$V_e = C_b^e \, V_b \tag{1}$$

where, C_b^e is a transformation matrix, which is computed with the attitude data measured by the attitude sensor (Lammas et al., 2007).

$$C_b^e = \begin{bmatrix} c\psi c\theta & -s\psi c\theta + c\psi s\theta s\phi & s\psi s\phi + c\psi c\phi s\theta \\ s\psi c\theta & c\psi c\phi + s\phi s\theta s\psi & -c\psi s\phi + s\theta s\psi c\phi \\ -s\theta & c\theta s\phi & c\theta c\phi \end{bmatrix} \tag{2}$$

where, s. = sin (.), c. = cos (.) and t. = tan (.), roll (φ), pitch (θ) and Yaw (ψ) or attitude/Euler angles of the underwater vehicle and V_b is the body frame velocity matrix [V_x, V_y, V_z] and V_e is the Earth frame velocity [V_n, V_e, V_d] matrix.

The vehicle velocity computed in the Earth frame coordinates is integrated over a time Δt to get the updated position every one second in geo-coordinates represented in latitude and longitude computed using Equations (3) and (4), which takes into account

https://doi.org/10.1017/S0373463315001058 Published online by Cambridge University Press

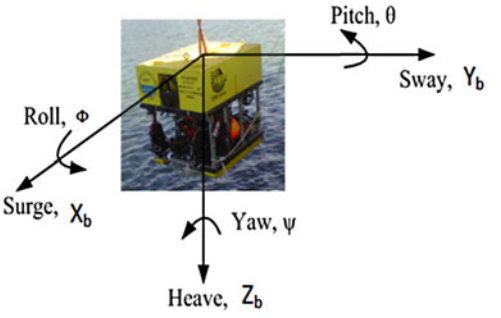

Figure 2. Representation of a typical vehicle orientation in the body frame.

for the Earth parameters (Liansheng and Tao, 2011; Titterton and Weston, 2004; Christensen et al., 2008; Hofmann-Wellenhof et al., 2011) shown in Equations (5) and (6).

$$Latitude\ L = L + \left(\frac{v_N * \Delta t}{R_N}\right) \tag{3}$$

$$Longitude\ \lambda = \lambda + \left(\frac{v_E * \Delta t * secL}{R_E}\right) \tag{4}$$

where, V_N is the Northing velocity of the vehicle in m/s; V_E is the Easting velocity of the vehicle in m/s; R_N is the meridian radius curvature of the Earth, R_E is the transverse radius curvature of the Earth computed as per the following Equations (5), (6), (7), (10) and Δt is the integration time of one second.

$$R_N = \left(\frac{R_E(1-e^2)}{(1-e^2 sin^2 L)^{\frac{3}{2}}}\right) \tag{5}$$

$$R_E = \left(\frac{R_E}{(1-e^2 sin^2 L)^{\frac{1}{2}}}\right) \tag{6}$$

The Earth parameters can be defined as per the international standard World Geodetic System (WGS).WGS84 (Grewal et al., 2001) is a reference Earth model as an ellipsoid. The Radius of the Earth, $R_E = 6378137$m, eccentricity, $e = 0.00335281066475$

3. SELECTION OF THE SENSOR SUITE USING A SIMULATOR. The selection of suitable navigational sensors is a key challenge in the design of underwater position estimation systems, as the accuracy of the position estimation depends mainly on the sensor characteristics (Fossen, 2012; Foss and Meland, 2007). Hence, based on the accuracy requirements of the mission, the navigational sensors are selected. A modelling and simulation tool was developed in MATLAB software, which accepts the initial position, sensor characteristics and mission profile as inputs, and provides the estimated position in the time domain as the output is used (Ramadass et al., 2013). The tool, which is coded with the error models of the DVL and attitude sensor, is explained below.

https://doi.org/10.1017/S0373463315001058 Published online by Cambridge University Press

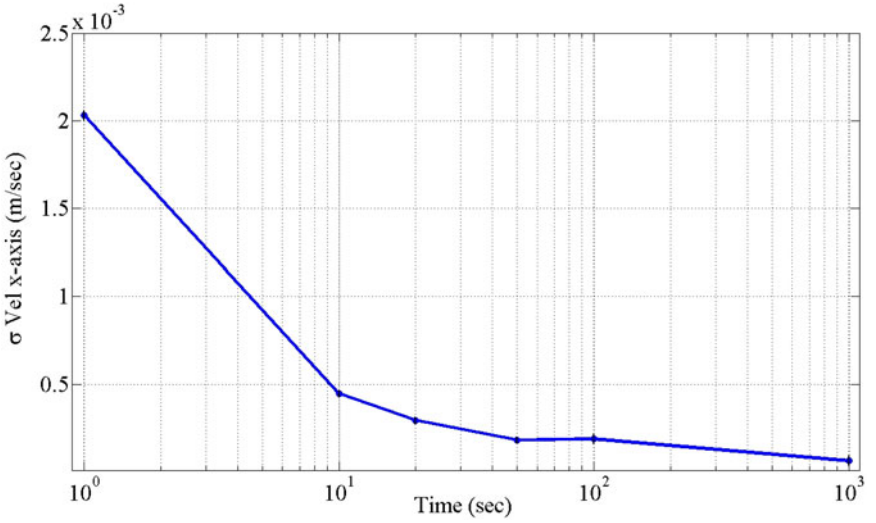

Figure 3. Analysis of the white noise characteristics for the DVL sensor using Allan Variance.

3.1. *Attitude sensor error model.* The vehicle's angular orientation in three axes is measured, using the attitude sensor housing compass and tilt sensors. The compass measures the vehicle heading with respect to true North and the tilt sensors provide the roll and pitch values. The error model of the attitude sensor is based on the following Equation (7) representing the bias error and random noise (Cruz et al., 2003; Healey et al., 1998; Foss and Meland, 2007; PNI sensors Corporation, 2014) parameters.

$$Heading\ \Psi_o = (\Psi_i * \sec L) + (\Psi_{acc} * b(t)) \tag{7}$$

$$Roll\ \Phi_o = \Phi_i(1 + S_f) + b(t) \tag{8}$$

$$Pitch\ \theta_o = \theta_i(1 + S_f) + b(t) \tag{9}$$

where, Ψ_i is the input heading measurement from the compass; Ψ_{acc} is the heading accuracy; Ψ_o is the heading output as shown in Equation (7). Φ_i is the input roll measurement from the tilt sensor; S_f is the scale factor; Φ_o is the roll output as shown in Equation (8). θ_i is the input pitch measurement from the tilt sensor; S_f is the scale factor and θ_o is the pitch output as shown in Equation (9). b(t) is the white Gaussian noise modelled with zero mean and the sensor standard deviation.

3.2. *Doppler Velocity Log error model.* The body frame velocity of the underwater vehicle is measured using the Doppler Principle, and the error model of the DVL is shown and explained in Equation (10):

$$V_o = (1 + S_f)V_i + b(t) \tag{10}$$

Where V_i is the simulated velocity input data from the DVL sensor, V_o is the velocity output from the model, S_f is the scale factor, and b(t) is the white Gaussian noise with zero mean and the sensor standard deviation (Jalving et al., 2004; Mandt et al., 2001; Braga et al., 2012; Teledyne RD Instruments, 2013; LinkQuest Incl, 2013, Hegrenaes et al., 2008) derived using the Allan Variance method as shown in Figure 3. The noise

https://doi.org/10.1017/S0373463315001058 Published online by Cambridge University Press

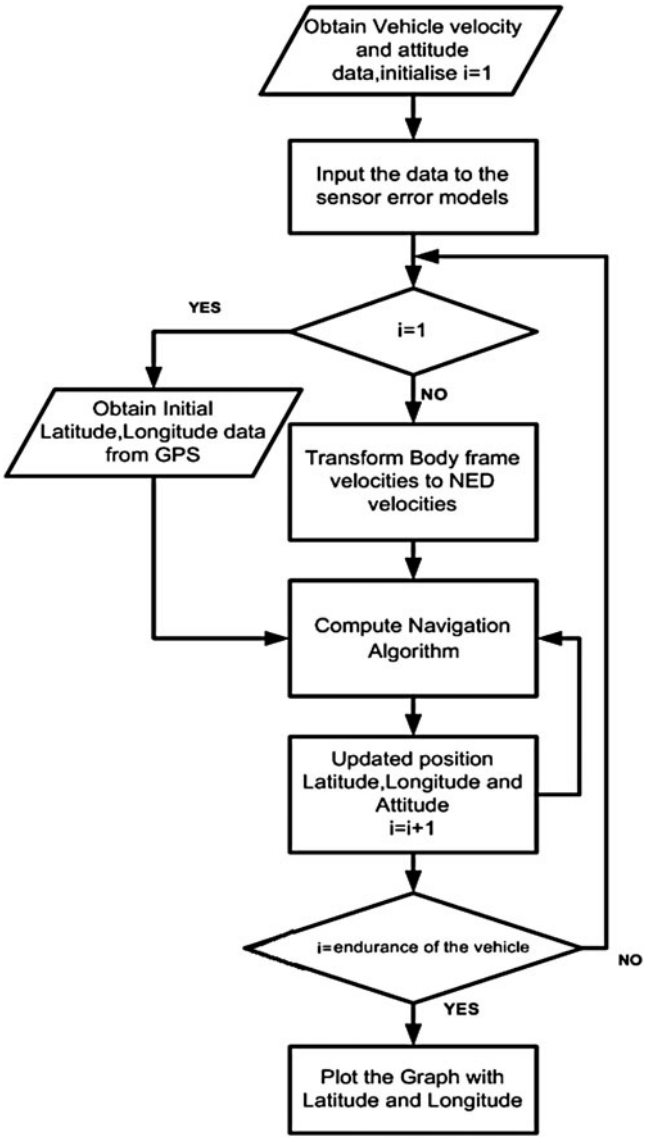

Figure 4. Simulation methodology.

characteristics of the DVL have been carried out by placing the DVL in a static mode in the NIOT in-house tank facility continuously for two hours and logging the data in a computer every second. Using the velocity data from the DVL, the Allan Variance graph (Allan, 1966; Hou, 2004; El-Sheimy et al., 2008) is plotted in Figure 3. It can be seen from Figure 3 that when the time is less than 10 seconds, the slope is −1/2 representing the white noise variance of 0·002 at one second.

3.3. *Simulation methodology.* Figure 4 explains the principle of the simulator software developed in MATLAB. In the simulation it is considered that the entire

https://doi.org/10.1017/S0373463315001058 Published online by Cambridge University Press

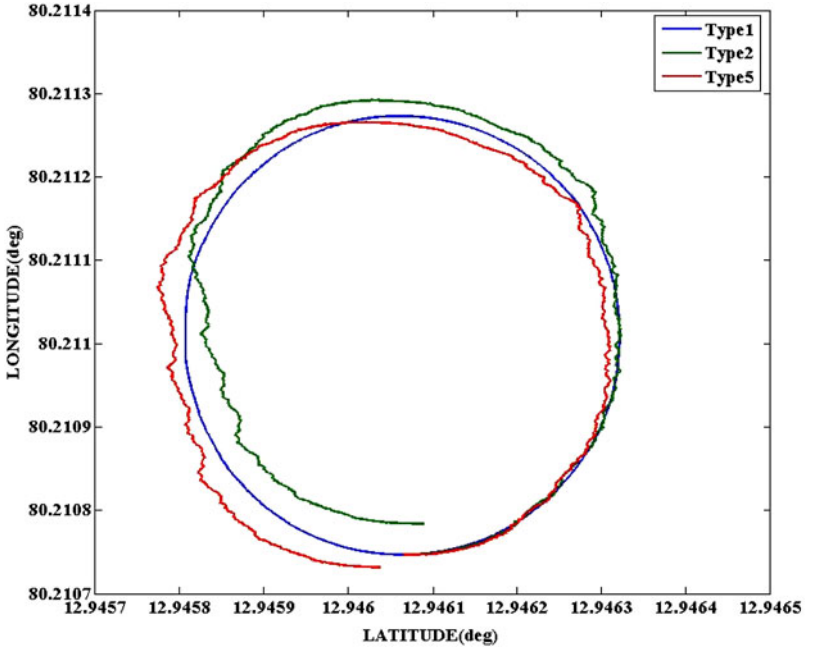

Figure 5. Simulation results for the sensor suites.

sensor data update rate is at one second. Based on the described sensor error models, three-axes body frame velocity and three-axes attitude, the sensor data is generated and stored as data files as per the designed circular vehicle trajectory (Ramadass et al., 2013). The initial position of the vehicle in latitude and longitude will be obtained from the GPS receiver, which is a standalone system with a fixed antenna, providing the position output in geo-coordinates using the GPS satellite constellation (Acquaris, 2012) in the National Marine Electronics Association (NMEA 0183) $GPGGA format.

The Earth parameters are initialised as per the WGS84 standard. The body frame velocities of the DVL are transformed into the Earth frame using a direct cosine matrix as explained in Equation (1) with Euler angles. The position estimation is done based on the navigation Equations (3)–(6) in the dead reckoning mode. The simulation algorithm computes and plots the position of the vehicle in geo-coordinates over the mission period for the given vehicle trajectory.

3.4. *Selection of the sensor suite.* The navigational system developed for the 500 m depth rated ROV demands a position estimation accuracy of better than 10 m in both the latitude and longitude coordinates, when the vehicle is operated with an average velocity of one knot, for a period of 30 minutes. In order to meet the defined mission requirements, a combination of the sensor suite with a range of commercially available DVL (Braga et al., 2012; Panish and Taylor, 2011; de Morais et al., 2013; Mandt et al., 2001) and attitude sensors (PHINS, 2013; PNI sensors Corporation, 2014; Honeywell magnetic sensors, 2014) was selected as three different types. Types 1, 2 and 3 represent the sensor suite with a highly accurate velocity log and different attitude sensors and types 4, 5 and 6 represent a less accurate velocity log and

https://doi.org/10.1017/S0373463315001058 Published online by Cambridge University Press

Table 1. Performance of the various combinations of sensor suites.

Suite	DVL	Attitude sensor	Shift from Lat after 30 min	Shift from Lon after 30 min
	Accuracy as % of velocity(cm/s)	accuracy(°/hr)	(m)	(m)
Type 1	0·3 ± 0·2	0·01	0·9	0·9
Type 2		0·8	2·2	2·22
Type 3		5·0	10·51	4·35
Type 4	1·1 ± 1·0	0·01	1·5	1·5
Type 5		0·8	5·1	5·15
Type 6		5·0	11·52	8·23

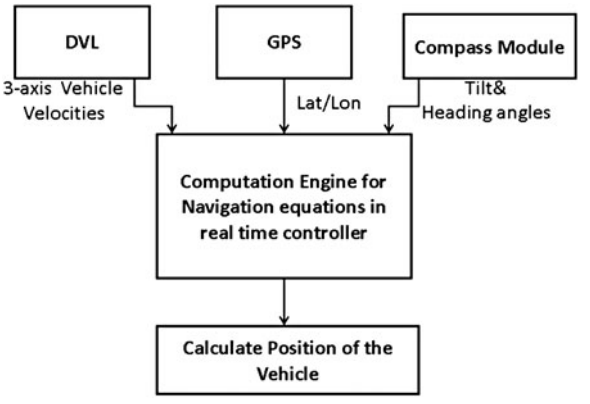

Figure 6. Architecture of the navigation system.

different attitude sensors. The performance of the sensor suite was simulated for the position estimation performance for the defined mission.

The simulation results for sensor suite types 1, 2 and 5 plotted in the geographical coordinates are shown in Figure 5. Details of the sensors considered in each suite and their simulated position estimation performances are shown in Table 1.

From the simulation results shown in Table 1, it can be seen that sensor suites 2 and 5 were found to match the target position estimation performance for the mission. By considering the overall project requirements, the type 5 sensor suite is identified for developing the vehicle's navigational system as it is low cost, small size and low weight and thus suitable for a shallow water ROV.

4. SYSTEM DEVELOPMENT AND EMULATOR-BASED VALIDATION.

Based on the simulation results, the navigational system is developed. The architecture of the hardware is shown in Figure 6 and the details of the interface are shown in Table 2.

The developed navigational system is qualified for its position estimation performance, using an in-house developed emulator. The emulator comprises a GPS-aided

https://doi.org/10.1017/S0373463315001058 Published online by Cambridge University Press

Table 2. Description of the hardware used for the navigational system.

Hardware	Accuracy description	Interface protocol and update rate
GPS	±5 m	RS232/1s
DVL	1·1% ± 1·0 cm/s	RS232/1s
Compass	0·8°	RS232/1s
Depth	±0·005	RS232/1s

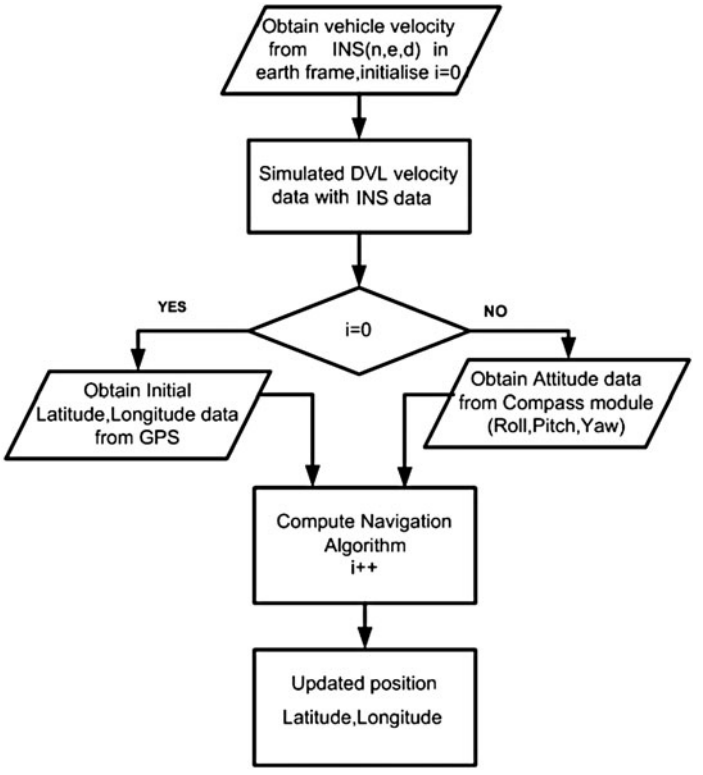

Figure 7. Performance validation algorithm using emulator.

high precision FOG-based INS (PHINS, 2013) providing attitude and velocity sensor inputs, which are fed to the software coded to introduce inaccuracies resembling the selected sensor suite. The GPS-aided FOG-based INS has a proven high precision performance with a heading stability accuracy of 0·002°/ hour and velocity accuracy of 0·01 m/s.

The output of the emulator module thus matches the output performance of the selected sensor suite. The emulator output is provided as input to the developed navigational system. Figure 7 shows the methodology involved in providing the emulation inputs and validating the position estimation performance of the navigational system. The developed navigational system is qualified for performance using the emulator-fed system by moving in a terrestrial vehicle in a known location (Latitude - 12·94621, Longitude - 80·21350) which can be seen in Figure 8. The terrestrial vehicle is

https://doi.org/10.1017/S0373463315001058 Published online by Cambridge University Press

Figure 8. Test setup for performance test using the emulation.

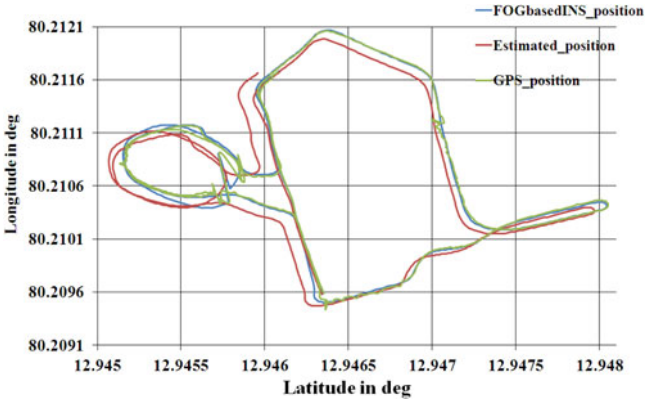

Figure 9. System's navigation performance using the emulator.

Table 3. Performance of the system compared with near ideal reference.

	Distance travelled		Location offset from ideal	
Time	GPS-aided FOG based-INS(in m)	Emulated system(in m)	Lat (in m)	Lon (in m)
To	0	0	0	0
To + 5 min	140	134·7	3·3	4·3
T0 + 10 min	146	144·2	5·5	8·6
T0 + 20 min	209·4	210·4	13·3	2·1
To + 30 min	229·5	228·5	13·3	3·2

manoeuvred in a profile almost resembling the expected underwater mission profile conditions (X and Y linear DOF and all three angular DOF).

Figure 9 shows the navigation plot of the GPS-aided FOG based-INS and the output of the emulator fed developed navigational system. Table 3 details the temporal

https://doi.org/10.1017/S0373463315001058 Published online by Cambridge University Press

performance of the emulator-fed navigational system with reference to the GPS-aided FOG-based INS.

5. IMPLEMENTATION AND PERFORMANCE IN SHALLOW WATER

ROV. The developed navigational system comprising attitude sensors, DVL and controller is mounted on board the 500 m depth rated ROV (Vedachalam at al., 2015). The vehicle velocity measurement using the DVL is based on the Doppler acoustic principle, which provides three-axes linear velocity data at an update rate of one second to the position estimation algorithm. Due to the vehicle dynamics, there are possibilities that could result in data outages from the DVL that could lead to erroneous position computation. To overcome the system's degraded performance during such data outages, a linear Kalman Filter (KF) is developed and incorporated in the DVL velocity measurements (Leader, 1994; Anonsen and Hallingstad, 2007; Welch and Bishop, 1995; Simon, 2006; Mandt et al., 2001). The prediction methodology of the KF is shown below.

The KF matrices for the estimation of velocities are given below.

A, is the state transition matrix linking the states at time k-1 and k-

$$A = [\boldsymbol{I}]_{3*3}$$

B, is the control input vector matrix

$$B = [\boldsymbol{O}]_{3*3}$$

u_{k-1}, is the input vector

$$u_{k-1} = [\boldsymbol{O}]_{1*3}$$

$\hat{X}_{k-1}$, is the *a priori* state vector at time k

$$\hat{X}_{k-1} = [\boldsymbol{O}]_{3*3}$$

H_k, is the measurement matrix

$$H = [\boldsymbol{I}]_{3*3}$$

Q is the process noise covariance

$$Q = 0.01^2 * [\boldsymbol{I}]_{3*3}$$

R is the measurement noise covariance

$$R = 0.52^2 * [\boldsymbol{I}]_{3*3}$$

P_k^-, is the covariance matrix of the prediction error initialised as

$$P_{k-} = 0.01 * [\boldsymbol{I}]_{3*3}$$

Z_k, is the measurement vector at time k

$$Z_k = H * V_k$$

where V_k is the linear vehicle velocity Input data in 3-axes from the DVL,

$$V_k = [\, v_x \quad v_y \quad v_z \,]$$

https://doi.org/10.1017/S0373463315001058 Published online by Cambridge University Press

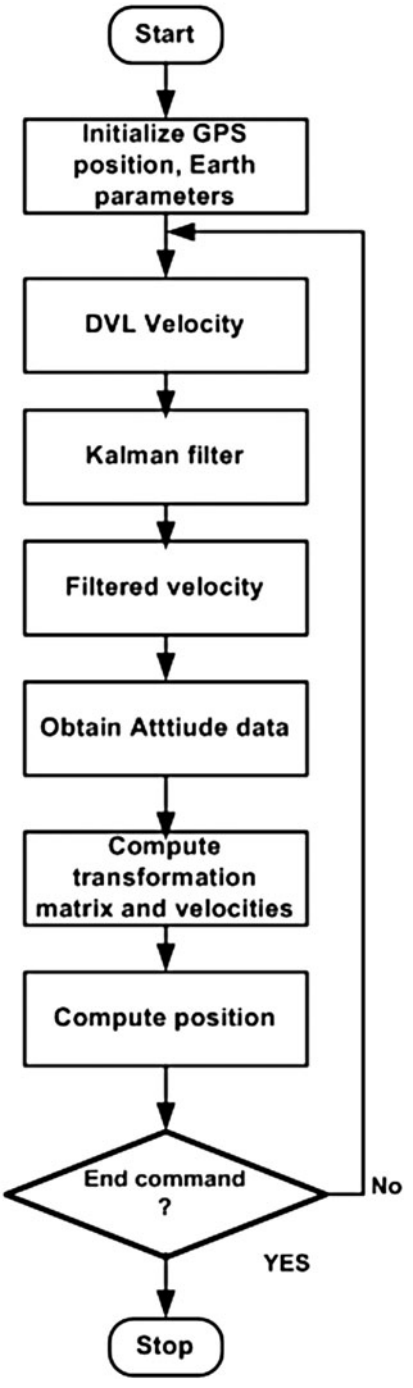

Figure 10. Implemented algorithm incorporating KF.

https://doi.org/10.1017/S0373463315001058 Published online by Cambridge University Press

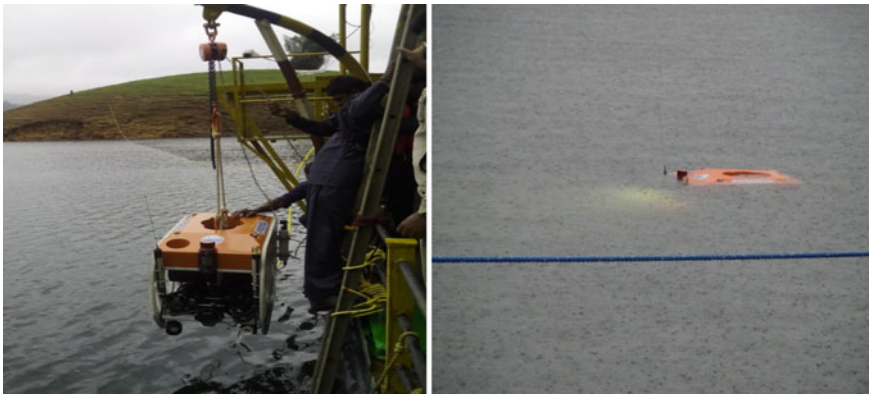

Figure 11. Navigational system tested for performance.

Time Update

$$\hat{X}_{k-} = A \quad \hat{X}_{k-1} + Bu_{k-1} \tag{11}$$

$$P_{k-} = AP_{k-1}A^T + Q \tag{12}$$

Measurement Update

$$K_k = P_k^- H^T (HP_k^- H^T + R)^{-1} \tag{13}$$

$$\hat{X}_k = \quad \hat{X}_{k-} + K(Z_k - H \quad \hat{X}_{k-}) \tag{14}$$

$$P_k = (I - K_k H_k)\, P_k^- \tag{15}$$

Where $\hat{X}_{k-}$ is the *posteriori* state vector at time k, K_k is the Kalman gain and P_k is the covariance of the *posterior* error.

Based on the Equations (11)–(15), the velocities measured from the DVL are taken as the input matrix, H_k and the process and measurement covariance parameters are tuned to filter the noisy velocity data. Based on standard KF tuning methods (Li et al., 2013; Healey et al., 1998), the filter is tuned to have a process noise covariance (Q) of 0·0001 and measurement noise covariance (R) of 0·2704, and the filtered velocities are obtained for the navigation algorithm computation. The implemented logic is shown in Figure 10.

As a part of the ROV qualification trials, Figure 11 shows the ROV being launched from the anchored barge in Idukki Lake in the Kerala State of South India, where the water depth at the test location was 40 m. The figure at right shows the vehicle operation, and the data is logged in the pilot console located on board the anchored barge (Vedachalam et al., 2015).

Figure 12 shows the vehicle velocity input for the position computation algorithm, without and with the KF in place.

The ROV was navigated for a period of 30 minutes at an average depth of 25 m and the recorded depth plot in the pilot console is shown in Figure 13.

Figure 14 shows the position plot of the underwater vehicle in geo-coordinates during the test period. It can be seen that the vehicle has navigated a distance of 120 m and at a maximum speed in x-axis to 0·5 m/s and y-axis to 0·115 m/s to

https://doi.org/10.1017/S0373463315001058 Published online by Cambridge University Press

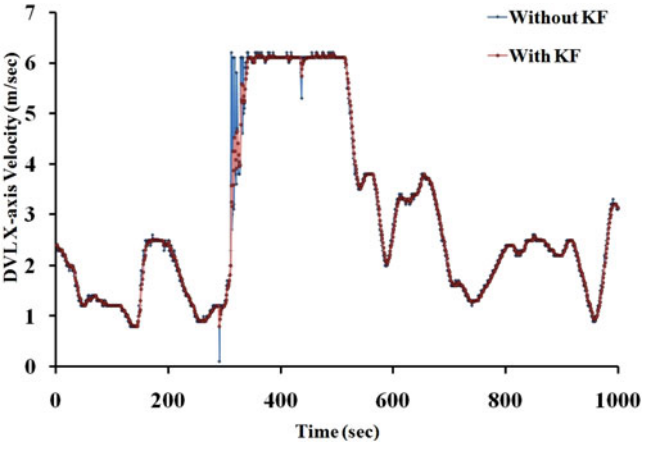

Figure 12. KPA performance for velocity during DVL outages.

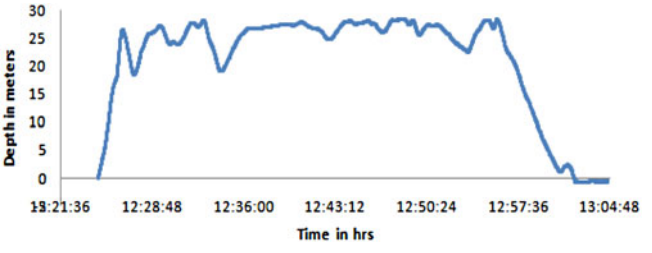

Figure 13. Depth plot for underwater navigation.

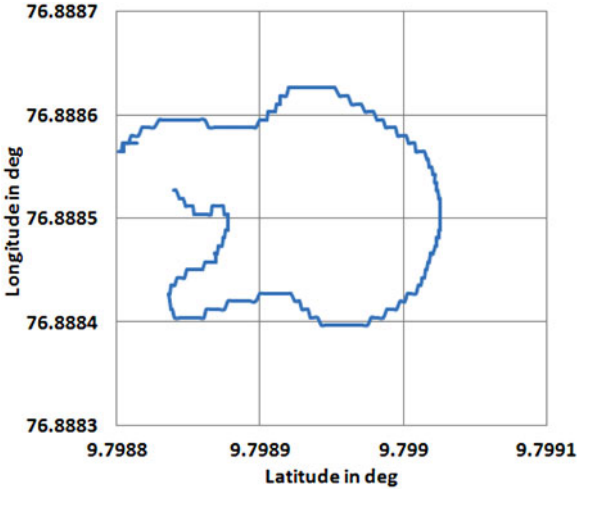

Figure 14. Geo-referenced plot of underwater navigation.

https://doi.org/10.1017/S0373463315001058 Published online by Cambridge University Press

perform a circular trajectory. After the 30 minute period, when the vehicle surfaced and was recovered to the stationary anchored barge, it could be seen that there were position offsets of 2·89 m in Latitude and −4·38 m in the longitude coordinates with resultant offset of 5·2 m and the calculated position error was 4·3%.The result is found to comply with the emulated performance with a position error of less than 5% which meets the mission requirements.

6. CONCLUSION. This paper has presented the navigational system developed for the position estimation of a shallow water Remotely Operated Vehicle using attitude and the Doppler Velocity Log with an initial position aid from GPS. Based on the defined vehicle position accuracy requirement of less than 10 m in the Latitude and Longitude coordinates for 30 minutes at one knot vehicle speed, suitable velocity and attitude sensors are identified using the in-house developed simulator tool. The position estimation performance of the developed system was validated using a precision emulator providing attitude and velocity sensor inputs with accuracies resembling the selected sensor suite, and was found to comply with the simulation results. The developed system was found to perform with the envisaged accuracy of less than 5%, when tested in the in-house developed shallow water Remotely Operated Vehicle. In the near future, it is planned to test the ROV in deeper waters and for longer mission durations, to test the position accuracy and improve the navigation algorithm.

ACKNOWLEDGEMENT

The authors gratefully acknowledge the support extended by the Ministry of Earth Sciences, Government of India, in funding this research. The authors also wish to thank the other staff involved in the project for their contribution and support.

REFERENCES

Acquaris. (2012). Acquaris Model, Astech Thales GPS receiver. http://ashgps.com/mirror/20130710/Marine%20Survey/Aquarius-Sagitta-3011/Manuals/Sagitta%20Seismic.pdf. Accessed 15 December 2012.

Allan, D. W. (1966). Statistics of atomic frequency standards. *Proceedings of the IEEE*, **54**(2), 221–230.

Anonsen, K. B., and Hallingstad, O. (2007). Sigma point Kalman filter for underwater terrain-based navigation. *Proceedings of the IFAC Conference on Control Applications in Marine Systems, Bol, Croatia*. (pp. 106–110).

Braga, J., Healey, A. J., and Sousa, J. (2012). Navigation scheme for the LSTS SEACON vehicles: Theory and application. In *Navigation. Guidance and Control of Underwater Vehicles*, **3**(1), 69–75).

Christensen, R., Fogh, N., la Cour-Harbo, A., and Bisgaard, M. (2008). *Inertial navigation system*. Department of Control Engineering in Aalborg University.

Cruz, N., Matos, A., de Sousa, J. B., Pereira, F. L., Silva, J., Silva, E., and Dias, E. B. (2003). Operations with multiple autonomous underwater vehicles: the PISCIS project. In *Second Annual Symposium on Autonomous Intelligent Networks and Systems AINS*.

de Morais, F. B. (2013). An Advanced Navigation System for Remotely Operated Vehicles. Department of Engineering Cybernatics, Norwegian University of Science and Technology (NTNU).

El-Sheimy, N., Hou, H. and Niu, X. (2008). Analysis and modeling of inertial sensors using Allan variance. *Instrumentation and Measurement, IEEE Transactions on*, **57**(1), 140–149.

Ellingsen, H. (2008). Development of a Low-Cost Integrated Navigation System for USVs. *Department of Engineering Cybernetics, Norwegian University of Science and Technology, Trondheim, Norway.*

Fallon, M. F., Papadopoulos, G., Leonard, J. J. and Patrikalakis, N. M. (2010). Cooperative AUV navigation using a single maneuvering surface craft. *The International Journal of Robotics Research*, **29**(12), 1461–1474.

Foss, H. T. and Meland, E. T. (2007). Sensor Integration for Nonlinear Navigation System in Underwater Vehicles. Department of Engineering and Cybernetics, Norwegian University of Science and Technology (NTNU).

Fossen, T.I. (1994). *Guidance and Control of Ocean Vehicles*, John Wiley.

Fossen, T.I. (2012). Low-cost integrated navigation systems for autonomos underwater vehicles. *Plenary paper presented at the XXXIII Jornadas de Automatica, Vigo, Spain*.

Geng, Y., Martins, R., and Sousa, J. (2010). Accuracy analysis of DVL/IMU/magnetometer integrated navigation system using different IMUs in AUV. In *Control and Automation (ICCA), 2010 8th IEEE International Conference on* (pp. 516–521). IEEE.

Grewal, M. S., Weill, L. R. and Andrews, A. P. (2001). *Global positioning systems, inertial navigation, and integration*. John Wiley & Sons.

Healey, A. J., An, E. P. and Marco, D. B. (1998). Online compensation of heading sensor bias for low cost AUVs. In *Autonomous Underwater Vehicles, 1998. AUV'98. Proceedings Of The 1998 Workshop on Underwater Navigation* (pp. 35–42). IEEE.

Hegrenaes, O., Berglund, E. and Hallingstad, O. (2008). Model-aided inertial navigation for underwater vehicles. *Robotics and Automation, ICRA 2008. IEEE International Conference on* (pp. 1069–1076), Pasadena, CA, USA.

Hofmann-Wellenhof, B., Legat, K. and Wieser, M. (2011). *Navigation: principles of positioning and guidance*. Springer Science & Business Media.

Honeywell magnetic sensors. (2014). http://www51.honeywell.com/aero/common/documents/myaerospacecatalog-documents/Missiles-Munitions/HMC6343.pdf. Accessed 20 January 2014.

Hou, H. (2004). *Modelling inertial sensors errors using Allan variance*. University of Calgary, Department of Geomatics Engineering, University of Calgary, Alberta.

Jalving, B., Gade, K., Hagen, O. K. and Vestgard, K. (2003). A toolbox of aiding techniques for the HUGIN AUV integrated inertial navigation system. In *OCEANS 2003. Proceedings* (Vol. **2**, pp. 1146–1153). IEEE.

Jalving, B., Gade, K., Svartveit, K., Willumsen, A. and Sorhagen, R. (2004). DVL velocity aiding in the HUGIN 1000 integrated inertial navigation system. *Modelling Identification and Control*, **25**(4), 223–236. Nice, France.

Lammas, A. K., Sammut, K. and He, F. (2007). A 6 DoF navigation algorithm for autonomous underwater vehicles. In *OCEANS 2007-Europe* (pp. 1–6). IEEE.

Leader, D.E. (1994). Kalman Filter Estimation of Underwater Vehicle Position and Attitude Using a Doppler Velocity Aided Inertial Motion Unit, Engineer Degree Thesis, *Massachusetts Institute of Technology and Woods Hole Oceanographic Institution*, Massachusetts, September 1994.

Li, W. and Wang, J. (2013). Effective adaptive Kalman filter for MEMS-IMU/magnetometers integrated attitude and heading reference systems. *Journal of Navigation*, **66**(1), 99–113.

Li, W., Wu, W., Wang, J. and Lu, L. (2013). A fast SINS initial alignment scheme for underwater vehicle applications. *Journal of Navigation*, **66**(2), 181–198.

Liansheng, L. and Tao, J. (2011). Research on Strap-down Inertial Navigation System Simulation. *Intelligent Computation Technology and Automation (ICICTA), 2011 International Conference on* (Vol. 2, pp. 1168–1171). IEEE.

LinkQuest Incl. (2013). http://www.link-quest.com/html/NavQuest600M.pdf. Accessed on 5th January 2013.

Mandt, M., Gade, K. and Jalving, B. (2001). Integrating DGPS-USBL position measurements with inertial navigation in the HUGIN 3000 AUV. *Proceedings of the 8th Saint Petersburg International Conference on Integrated Navigation Systems, Saint Petersburg, Russia*.

Marco, D. B. and Healey, A. J. (2001). Command, control, and navigation experimental results with the NPS ARIES AUV. *IEEE Journal of Oceanic Engineering*, **26**(4), 466–476.

Narayanaswamy, V., Raju, R., Durairaj, M., Ananthapadmanabhan, A., Annamalai, S., Ramadass, G. A. and Atmanand, M. A. (2013). Reliability-Centered Development of Deep Water ROV ROSUB 6000. *Marine Technology Society Journal*, **47**(3), 55–71.

Panish, R. and Taylor, M. (2011). Achieving high navigation accuracy using inertial navigation systems in autonomous underwater vehicles. *OCEANS, 2011 IEEE-Spain* (pp. 1–7).

PHINS. (2013). Photonic Inertial Sensors, IXBLUE, France. https://www.ixblue.com/products/phins. Accessed 30 March 2013.

PNI sensors corporation. (2014) PNI sensors corporation. CA, USA. http://www.precisionnav.com/products/tcm. Accessed 25 January 2014

Ramadass, G. A., Vedachalam, N., Balanagajyothi, V., Ramesh, R. and Atmanand, M. A. (2013). A modeling tool for sensor selection for inertial navigation systems used in underwater vehicles. *Ocean Electronics (SYMPOL), 2013* (pp. 175–188). IEEE. Kochi, India.

Simon, D. (2006). *Optimal state estimation: Kalman, H infinity, and nonlinear approaches*. John Wiley & Sons.

Teledyne RD Instruments. (2013). http://www.rdinstruments.com/pdfs/wh_navigator_ds_lr.pdf. Accessed 20 January 2013

Titterton, D.H. and Weston, J.L. (2004). *Strapdown inertial navigation technology*. The Institution of Electrical Engineers (pp. 344–345).

Vedachalam, N., Ramadass, G. A. and Atmanand, M. A. (2014a). Reliability centered modeling for development of deep water Human Occupied Vehicles. *Applied Ocean Research*, **46**, 131–143.

Vedachalam, N., Ramadass, G. A. and Atmanand, M. A. (2014b). Review of Technological Advancements and HSE-Based Safety Model for Deep-Water Human Occupied Vehicles. *Marine Technology Society Journal*, **48**(3), 25–42.

Vedachalam, N., Ramesh, S., Subramanian, A. N., Sathianarayanan, D., Ramesh, R., Harikrishnan, G. and Atmanand, M. A. (2015). Design and development of Remotely Operated Vehicle for shallow waters and polar research. In *Underwater Technology (UT), IEEE* (pp. 1–5). Chennai, India.

Welch, G. and Bishop, G. (1995). *An introduction to the Kalman filter. Department of Computer Science, University of North Carolina at Chapel Hill, Chapel Hill, NC*.